Online Human Walking Imitation in Task and Joint Space based on Quadratic Programming

Kai Hu, Christian Ott and Dongheui Lee

***Abstract*— This paper presents an online methodology for imitating human walking motion of a humanoid robot in task and joint space simultaneously. Two aspects are essential for a successful walking imitation: stable footprints represented in task space and motion similarity represented in joint space. The human footprints are recognized from the captured motion data and imitated by the robot through conventional zero-moment point (ZMP) control scheme. Additionally we focus on similar knee joint trajectories for the motion similarity, which are related to knee stretching and swing leg motion. The inverse kinematics suffers from three problems: knee singularity, strongly conflicting tasks and underactuation. We formulate this problem as a quadratic programming (QP) with dynamic equality and inequality constraints. The discontinuity of dynamic task switching is solved by introducing an activation buffer, resulting in a cascaded QP form. Finally we evaluate the effectiveness of the proposed approach on the DLR humanoid robot TORO.**

I. Introduction

The goal of humanoid research is to develop humanoid robots that can work as human in our daily life. Therefore humanoid robots are expected to behave like human, which could achieve expressive and meaningful motions, enhance its acceptance in the human environment and therefore improve the human robot interaction. However the meaning of human-like motion is related to the motion kinematics, dynamics as well as subjective feelings in different scenarios and it is difficult to formulate a general definition.

Recently methods based on human motion capturing to generate feasible human-like motions for humanoid robots have drawn great attention in robotics community. In the context of motion imitation, target systems usually have similar kinematic structures as human and it is straightforward to define human-like motion as having similar joint or task space configurations. The quality of the imitation depends greatly on the selection of appropriate corresponding targets. This paradigm has been proven to be efficient and effective by many research works [1], [2], [3], [4], [5], [6]. The motion similarity of upper-body part has been well demonstrated by both task and joint space mapping in kinematic level. However lower-body motions are either omitted or limited to slow stepping without consideration of motion similarity.

In this work we focus on online generating human-like walking motions from captured human motion data for a humanoid robot. The walking imitation is considered with two aspects: footprint imitation in task space and motion similarity in joint space. The human footprints are recognized from the captured motion data and imitated through conventional ZMP control scheme, which results in a non human-like walking behavior with similar footprints as human. The motion similarity is considered to have similar joint trajectories which results in similar leg motions. Finally the walking imitation problem is formulated by a set of task and joint space tracking targets with different priorities. Since the task and joint space targets are usually conflicting strongly with each other, we introduce dynamic target activation during different walking phases. Because of the limitation of the robot's degrees of freedom (DOFs) and the kinematic difference of the feet, we focus particularly on achieving similar knee joint trajectories, which results in knee stretched walking and human-like swing leg motions. We formulate our walking control problem as a quadratic programming in order to avoid the knee singularity explicitly by inequality constraints. Dynamic constraint is introduced to resolve conflicting tasks during different walking phases. A continuous control law is achieved by adding an activation buffer during constraint switching.

The rest of the paper is organized as follows. Related works are discussed and compared in Section II. In Section III procedures of walking motion recognition from human motion data and pattern generation based on ZMP preview

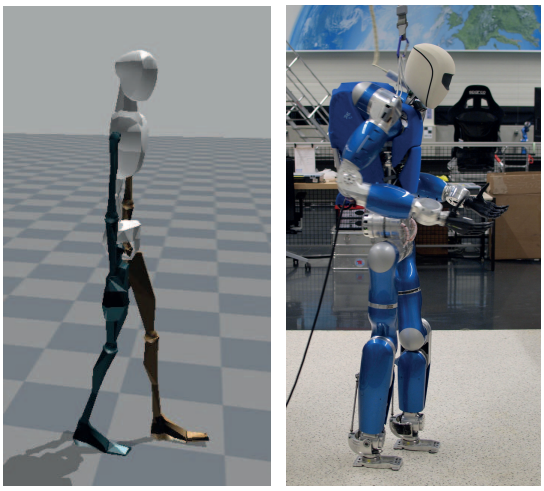

Fig. 1. Humanoid robot TORO imitates the human walking motion with foot prints imitation and knee joint tracking. Note that only lower body is controlled for imitation.

Kai Hu and Dongheui Lee are with the Department of Electrical Engineering and Information Technology, Technical University of Munich, D-80290 Munich, Germany. kai.hu@tum.de, dhlee@tum.de
Christian Ott is with the Institute of Robotics and Mechanics, German Aerospace Center (DLR), D-82234 Weißling, Germany. christian.ott@dlr.de

control are briefly introduced. We propose the walking imitation controller with knee joint mapping in Section IV. The experiment results on the DLR humanoid robot TORO are shown in Section V. Fig. 1 shows a preview of the walking imitation by TORO.

II. Related Works

Without considering the motion similarity, feasible walking motion was generated from human motion data by designing the ZMP trajectory based on a rolling foot model [7]. Online footprint imitation was realized on the MAHRU-R robot by feeding the recognized and adapted human step parameters into a classical ZMP based walking controller [8]. Instead of applying human motion data directly, some researchers have worked on human-like biped gait synthesis based on certain human walking characteristics. Harada et al. [9] extracted many human walking features in a parametric form from multiple human motion data and applied them to a ZMP-based pattern generator. Their major contribution is the reduction of the waist sway. Vertical waist motions are designed to achieve knee stretched walking behaviors in [10], [11], [12]. They focused on stretching the knee as much as possible within the singularity safe margin by lifting the waist. Compared with these methods, our approach avoids knee singularity explicitly and therefore can achieve more stretched knee configuration (5 degrees in this implementation). Moreover our algorithm can be solved online for different robots and different foot step motions while the above works rely on offline optimization and careful trajectory design based on the robot's specific leg geometry. Some research works also considered heel-down and toe-off motions during walking [12], [13]. Because most state of the art humanoid robots still have rigid flat feet without toe joints, we consider this part as future work when robot foot design becomes more biomimic.

Ogura et al. proposed an approach to realize the knee stretched walking with predefined knee trajectories by utilizing additional waist joints [13]. Their method requires redundant leg systems which restrict the application to general biped platforms. Our approach deals with the underactuation problem by introducing dynamic target switching in different walking phases instead of demanding more DoFs of the system. Fig. 2 shows an overview of the proposed walking imitation framework.

III. Walking Motion Recognition and Pattern Generation

There are several techniques available for the human motion capturing which is precise enough to do lower-body motion imitation, such as marker based optical motion sensor, inertial measurement unit and exoskeleton system. Cartesian data of different body segments are usually provided directly. Joint space trajectories can be easily calculated based on a simplified human skeleton model. We use both Cartesian and joint space data as the reference input of our imitation algorithm.

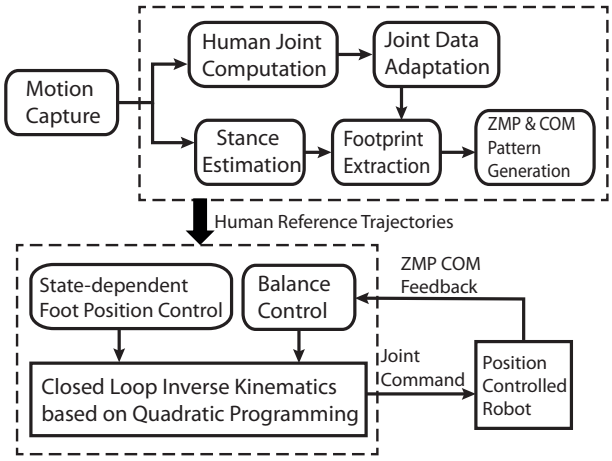

Fig. 2. Overview of the walking imitation framework with task and joint space mapping.

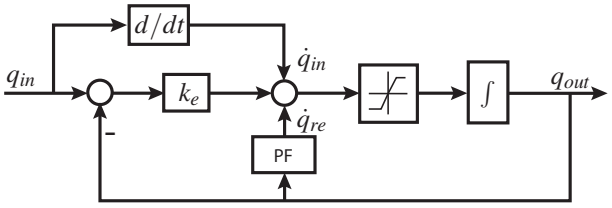

Fig. 3. Human joint trajectory adaptation using repulsive potential field and velocity saturation.

A. Human Joint Angle Adaptation

Before we use the human joint data for the joint space mapping, it is reasonable to check if they are consistent with the robot hardware limits. Additionally the minimal angle of the knee is set to be five degrees, which is selected as the limit value for singularity avoidance. The adaptation procedure is formulated as a joint tracking system (Fig. 3). We utilize the concept of potential fields to avoidance the joint limit. The repulsive joint velocity $\dot{q}_{re}$ is generated as an exponential function when the joint is approaching the limit:

$$\dot{q}_{re} = \begin{cases} k_1 e^{\frac{k2}{q-q_{min}}} & \text{for} \quad q \leq q_{min} + q_0 \\ 0 & \text{for} \quad q_{min} + q_0 < q < q_{max} - q_0 \\ -k_1 e^{\frac{k2}{q_{max}-q}} & \text{for} \quad q \geq q_{max} - q_0 \end{cases} \quad (1)$$

where q_{min} and q_{max} are lower and upper bounds of the joint position, q_0 is a positive start distance from where the potential field acts and k_1 and k_2 are positive parameters. The velocity limits are treated by simple saturation. The velocity discontinuity as the joint reaches the joint limit is treated by a position dependent velocity constraint in Section IV. In this study the adaptation procedure reduces the leg swing motion if human swings his leg too fast and ensures the minimal singularity robust knee angles in the reference trajectories.

B. Footprint Recognition

Based on the observation that the supporting foot velocity should stay within a predefined threshold value for a certain

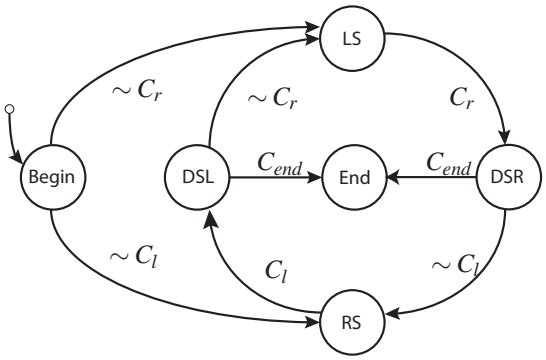

Fig. 4. Finite state machine for stance estimation. LS and RS are left and right single support states. DSL and DSR are separated double support states. C_r and C_l correspond to the support condition of the right and left leg respectively and $\sim$ represents the logic operation NOT.

time [8], we can judge the support state of each foot from foot velocities. Position data usually suffer from sensor drift and therefore are not suitable for the stance estimation. In order to prevent wrong estimation because of sensor noise we construct a finite state machine and design state transition conditions (Fig. 4).

We control the humanoid robot as a marionette by feeding the corresponding human joint angles into the robot forward kinematics model. In this way the task space targets are not related to the size of the robot. The next supporting foot position is then determined by extracting the relative feet position at the time of stance changes and adding it to the current supporting foot position. The walking turning angle can be extracted from human toe data directly. The foot swing trajectories are constructed by interpolation between via points which are taken time-uniformly from the foot trajectory of the joint mapping.

C. Pattern Generation

1) Reference ZMP Trajectory Planning: Without special equipment such as force plate it is hard to measure human's ZMP data online. Moreover mapping human's ZMP to the robot is difficult because there is a big gap of the dynamics properties between the two subjects. In this study we design the robot reference ZMP trajectory according to the footprints as follows:

- Single Support: The ZMP moves along the main axis of the supporting foot forward with a predefined velocity. The maximal ZMP displacement is bounded by the foot size. There is no displacement of the ZMP along the orthogonal direction of the main axis.
- Double Support: The ZMP jumps to the middle of the new supporting foot position at the beginning of the double support phase.

2) Reference COM Trajectory Generation: For walking pattern generation, simplified robot model is usually utilized to avoid complex multi-body dynamics computation. In this study the linear inverted pendulum model (LIPM) is taken as the simplified dynamics model of the humanoid robot

$$\boldsymbol{p} = \boldsymbol{c} - \frac{c_z}{g}\ddot{\boldsymbol{c}} \tag{2}$$

in which $\boldsymbol{p} = \begin{bmatrix} p_x & p_y \end{bmatrix}^T$ [1] is the ZMP position vector, $\boldsymbol{c} = \begin{bmatrix} c_x & c_y \end{bmatrix}^T$ the COM position vector, c_z the constant COM height and g the gravity constant. Despite its simplicity, the effectiveness of this model has been proven by many applications. We used the preview control scheme proposed by Kajita *et al.* [14] to compute the reference COM trajectory.

IV. Walking Imitation Control

Compared with conventional walking controller, we have additional tasks of joint space tracking for the motion similarity, which make the biped system underactuated. Moreover targets in task space and joint space usually conflicting strongly with each other, which means the tasks cannot be resolved together. Instead of requiring additional system DoFs, the concept of dynamic tasks is introduced to solve the problems. During different walking phases different tasks are activated or deactivated, which achieves a compromise between the dynamic stability and human motion similarity. We choose to formulate our walking control as a QP problem which gives us the benefit that we can consider inequality constraint explicitly. This gives us a good solution of the knee stretching singularity problem.

A. General Formulation of Redundant Inverse Kinematics

Conventional solution of redundant inverse kinematics is based on the pseudo-inverse of the Jacobian matrix. Lower priority tasks are projected into the null space of the higher priority tasks [15]. More generally it can be formulated as a constrained quadratic programming problem with equality and inequality constraints:

$$\begin{aligned} \arg\min_{\dot{\boldsymbol{q}}} \; & f(\dot{\boldsymbol{q}}) = \frac{1}{2}\dot{\boldsymbol{q}}^T \boldsymbol{H}\dot{\boldsymbol{q}} + \boldsymbol{C}\dot{\boldsymbol{q}} \\ \text{subject to} \; & \boldsymbol{J}\dot{\boldsymbol{q}} = \dot{\boldsymbol{x}} \\ & \boldsymbol{A}\dot{\boldsymbol{q}} \leq \boldsymbol{b} \end{aligned} \tag{3}$$

where $\boldsymbol{H} \in \mathbb{R}^{n \times n}$ is a positive definite cost matrix and $\boldsymbol{C} \in \mathbb{R}^n$ a linear cost vector. The high priority tasks can be regarded as equality constraints with $\boldsymbol{J}$ and $\dot{\boldsymbol{x}}$ while lower priority tasks can be considered in the cost function. One of the advantages of the QP form of inverse kinematics is that it allows inequality constraints explicitly, which are represented by $\boldsymbol{A}$ and $\boldsymbol{b}$. Researchers also proposed methods to assign priorities to inequality tasks [16].

B. Walking Imitation Control in QP form

We formulate the walking imitation control of the biped system as following QP problem:

[1] Throughout this paper, x denotes the forward walking direction, z is vertical direction (opposite to the gravity) and y is orthogonal to x and z.

$$
\begin{aligned}
\arg\min_{\dot{\boldsymbol{q}}} \; & f(\dot{\boldsymbol{q}}) = \omega_1 f_1 + \omega_2 f_2 + \omega_3 f_3 \\
& f_1 = \left\| \dot{\boldsymbol{x}}_{body,ori} - \boldsymbol{J}_{body,ori}\dot{\boldsymbol{q}} \right\|^2 \\
& f_2 = \left\| \dot{\boldsymbol{q}}_{knee} - \dot{\boldsymbol{q}}_{knee,human} \right\|^2 \\
& f_3 = \left\| \dot{\boldsymbol{x}}_{leg,xz} - \boldsymbol{J}_{leg,xz}\dot{\boldsymbol{q}} \right\|^2 \\
\text{subject to} \; & \boldsymbol{J}_{com,xy}\dot{\boldsymbol{q}} = \dot{\boldsymbol{x}}_{com,xy} \\
& \boldsymbol{J}_{leg,y,ori}\dot{\boldsymbol{q}} = \dot{\boldsymbol{x}}_{leg,y,ori} \\
\text{(dynamic)} \; & \boldsymbol{J}_{leg,xz}\dot{\boldsymbol{q}} = \dot{\boldsymbol{x}}_{leg,xz} \\
& \boldsymbol{A}_{knee}\dot{\boldsymbol{q}} \leq \boldsymbol{b}_{knee} \\
& \boldsymbol{A}_{com,z}\dot{\boldsymbol{q}} \leq \boldsymbol{b}_{com,z} \\
& \dot{\boldsymbol{q}}_{min} \leq \dot{\boldsymbol{q}} \leq \dot{\boldsymbol{q}}_{max}
\end{aligned}
\tag{4}
$$

The quadratic cost function consists of three terms: f_1 is the body orientation error; f_2 is the knee joint tracking term; f_3 represents the foot position error in x and z directions, which has conflict with the knee tracking targets. And $\{\omega_i | i = 1,2,3\}$ are weighting factors of each term respectively. They are selected according to the task importance (in our implementation $\omega_1 > \omega_2 > \omega_3$). The equality constraints correspond to the highest priority task which should be solved exactly. The foot positions in x and z directions are treated as dynamic targets by activating and deactivating the corresponding equality constraints in different walking phases. The inequality constraints contain the robot joint velocity bounds, the knee joint constraint and the COM vertical motion constraint which will be explained later. All the reference velocities are obtained through human motion processing in Section III except for $\dot{\boldsymbol{x}}_{com,xy}$, which is obtained through the feedback balance controller discussed later. In this study we keep the foot orientation always parallel to the ground during the swinging phase to avoid premature collisions between feet and ground. In each control time step, this QP problem is solved to obtain the desired joint velocities.

C. Knee Joint Constraint

Human stretches the knee joints fully during the walking. However in the neighborhood of robot's knee joint singularity, very large joint velocity is needed to achieve small Cartesian velocity, which will make the QP problem unsolvable because of the robot joint velocity limits. The knee singularity is avoided by setting a minimal angle of the knee joint. In the experiment we found $q_s = 5^\circ$ is an enough margin which makes the QP always solvable. We formulate this position limit in velocity level and combine it with the joint velocity limit

$$
\max\left[\dot{q}_{min,knee}, \frac{q_s - q_{knee}}{\Delta t}\right] \leq \dot{q}_{knee} \quad . \tag{5}
$$

The knee minimal position introduces unilateral constraints which results in joint velocity jumps when the knee joint reaches the limit. We solve this problem by changing the knee joint velocity constraints to a position dependent velocity constraint:

$$
\sqrt{2(q_{knee} - q_s)\ddot{q}_{knee,max}} \leq \dot{q}_{knee} \tag{6}
$$

in which q_{knee} is the current knee joint position and $\ddot{q}_{knee,max}$ is the maximal amplitude of the knee joint acceleration. With this constraint the joint velocity is always able to be reduced to zero from the current joint position with maximal joint acceleration. We can combine the knee joint constraints with the joint velocity lower bound to form one constraint:

$$
\begin{aligned}
& \max\left[\dot{q}_{min,knee}, (q_s - q_{knee})/\Delta t, \sqrt{2(q_{knee} - q_s)\ddot{q}_{knee,max}}\right] \\
& \leq \dot{q}_{knee}
\end{aligned}
\tag{7}
$$

D. Vertical COM Acceleration Constraint

The COM height motion is not controlled directly in our framework. The vertical COM motion could be generated by the supporting leg knee trajectory indirectly. Since our pattern generator is based on the LIPM, it is necessary to examine the ZMP error caused by the vertical COM motion. Without consideration of angular momentum the ZMP equation can be written as

$$
\boldsymbol{p}' = \boldsymbol{c} - \frac{z}{\ddot{z} + g}\ddot{\boldsymbol{c}} \tag{8}
$$

where z is the changing COM height. The ZMP error introduced by the COM height motion in x direction can be calculated by subtracting (8) from (2)

$$
e_{px} = p_x - p'_x = \frac{c_z\ddot{z} + g(c_z - z)}{g(\ddot{z} + g)}\ddot{x} \quad . \tag{9}
$$

It has been shown in [11] that the ZMP error is mainly determined by $\ddot{z}$. We want to limit our ZMP error to be small

$$
\left|e_{px}\right| \approx \left|\frac{c_z\ddot{z}}{g(\ddot{z} + g)}\ddot{x}\right| \leq e_{pxm} \tag{10}
$$

in which the e_{pxm} is the maximal magnitude of the ZMP error in x direction introduced by vertical COM motions. The value of e_{pxm} is determined by the maximal allowed deviation from the desired ZMP position to the foot edges, e.g. half of the foot length. After rearrangement we can get the limit of the COM height acceleration

$$
-\frac{e_{pxm}g^2}{c_z|\ddot{x}| + e_{pxm}g} \leq \ddot{z} \leq \frac{e_{pxm}g^2}{c_z|\ddot{x}| - e_{pxm}g} \quad . \tag{11}
$$

If we assume the maximal horizontal COM acceleration $\ddot{x}_m$ are known, which depends on the walking speed, we can replace $|\ddot{x}|$ with $\ddot{x}_m$ and get the strict limit of the COM height acceleration. The same calculation can be done also in y direction.

In order to include the acceleration constraints into the QP formulation, $\ddot{z}$ at time t may be approximated as:

$$
\ddot{z}(t) \approx \frac{1}{\Delta t}(\dot{z}(t) - \dot{z}(t - \Delta t)) \tag{12}
$$

By using (12) we can write the COM height acceleration constraint in velocity level:

$$\ddot{z}_{min}\Delta t + \dot{z}(t-\Delta t) \leq \dot{z}(t) \leq \ddot{z}_{max}\Delta t + \dot{z}(t-\Delta t) \tag{13}$$

in which $\ddot{z}_{min}$ and $\ddot{z}_{max}$ are the COM height acceleration limits obtained from (11).

E. Dynamic Targets for State-dependent Foot Control

The reason of separating the foot position control in x,z directions from y direction is due to the conflict between knee joint angle and foot Cartesian trajectories. The knee joint approximately determines the leg length and therefore the feet relative height. Also the x direction movement is closely related with the knee joint. We want to achieve stable foot contact while following the human knee joint trajectory as close as possible. A state-dependent foot position controller based on dynamic target switching is designed to achieve the goal.

1) Single Support: The single support phase is separated time-equally into two periods: swing phase and landing phase. In swing phase the foot height trajectory is determined by the knee trajectory of the human swing leg, aiming at achieving human-like swing motion. Therefore the dynamic targets of foot x and z direction are deactivated and the knee tracking target has good performance. At the beginning of the landing phase landing foot trajectory is generated from the current foot position and velocity through monotone cubic interpolation.The dynamic targets of foot x and z direction are activated in order to achieve a stable foot landing.

2) Double Support: The foot height has to be strictly regulated to achieve a stable foot contact in the beginning of double support. This is important for the transition of the robot ZMP. In this case we need to keep the dynamic targets activated and make the feet stay on the ground for maximal stability. Since both knee joints are almost stretched at the beginning of the double support, human moves his COM forward and maintains the double support by heel up motion and toe support. However the robot has flat feet and must have full contact between foot and ground, which leads to knee bending motion. This can be reduced by shortening the double support period.

3) Smooth Transition of Dynamic Targets: The activation and deactivation of the dynamic targets brings impacts into the system, which results in joint velocity jumps. The discontinuity of the joint velocities can be solved by introducing an activation buffer which smoothly activates or deactivates the dynamic targets. Instead of directly inserting or removing the corresponding equality constraints, we put the following constraint into the QP:

$$\boldsymbol{J}_{feet,xz}\dot{\boldsymbol{q}} = h\dot{\boldsymbol{x}}_{xz} + (1-h)\boldsymbol{J}_{feet,xz}\dot{\boldsymbol{q}}_{static} \tag{14}$$

in which h is activation parameter changes smoothly from 0 to 1 during task activation and 1 to 0 during task deactivation. Any smooth function can be used for designing the activation parameter, e.g. sinus function in our implementation. $\dot{\boldsymbol{q}}_{static}$ represents the QP solution with only static constraints. This treatment requires to solve an additional QP only with the static constraints during the switching.

F. Online Balance Control

The COM-ZMP feedback controller proposed by Choi *et al.* [17] is adopted as the online feedback balance controller, which should work against many existing disturbances in the real robot system. It has the following control law:

$$\begin{aligned} \boldsymbol{u} &= \dot{\boldsymbol{c}}_d - \boldsymbol{K}_p\boldsymbol{e}_p + \boldsymbol{K}_c\boldsymbol{e}_c \\ \boldsymbol{e}_p &= \boldsymbol{p}_d - \boldsymbol{p}_r \\ \boldsymbol{e}_c &= \boldsymbol{c}_d - \boldsymbol{c}_r \end{aligned} \tag{15}$$

where $\boldsymbol{u}$ denotes the control input for the COM velocity, $\dot{\boldsymbol{c}}_d$ is the reference COM velocity vector, $\boldsymbol{e}_p$ and $\boldsymbol{e}_c$ are ZMP and CoM error vector respectively. $\boldsymbol{p}_d$ and $\boldsymbol{c}_d$ are desired ZMP and COM positions. $\boldsymbol{p}_r$ and $\boldsymbol{c}_r$ are the real ZMP and COM positions calculated from the force torque sensors and joint encoders. The error gain matrices $\boldsymbol{K}_p$ and $\boldsymbol{K}_c$ should obey the stability condition given in [17].

V. Experiment Results

The proposed walking imitation approach is evaluated on the DLR humanoid robot TORO in the joint position control mode. The robot is about 1.6 meters high from foot to shoulder and the body weight is about 75kg. It has total 25 DoFs, including each leg 6 DoFs, each arm 6 DoFs and torso 1 DoF. In the experiment we only control the 12 DoFs of the legs and other joints are fixed as constant values. The robot has a rather compact foot size (95mm wide and 190mm long), which makes the balance control very challenging. In each foot a force/torque sensor is equipped to measure the ground reaction force for the calculation of the ZMP.

The human motion data is captured by Xsens MVN motion capture suit which is based on inertial sensors and has the ability to stream the motion data in real-time. A straight forward walking motion consisting of 8 steps performed by a young male person of 1.8 meters high is used for evaluating the effectiveness of the proposed approach (Fig. 5 (a)). The algorithm is not restricted only for straight walking imitation. The walking frequency is around 0.8sec/step and the human step length is around 35cm.

Our whole procedure runs online with a time delay of preview length 1.6s. We use an open source QP solver called qpOASES [18] for online calculation. We have conducted the experiment both in dynamics simulation (OpenHRP [19]) and on real robot platform. For real robot the cascaded QP form runs at 1000 Hz on the robot's one board real time linux system equipped with a recent intel i7 CPU. Due to the relative low joint velocity limit of the robot, the mapped step length can currently achieve 20cm on the robot with the same step frequency as human (Fig. 5 (c)). When we release the joint velocity constraints to larger values in the dynamic simulation, the simulation results show that the robot can also imitate the walking with a large step length as human (Fig. 5 (b)).

A. Motion Similarity

In this study the motion similarity is mainly evaluated by comparing the difference between human and robot knee angles. Two experiments (conventional and proposed

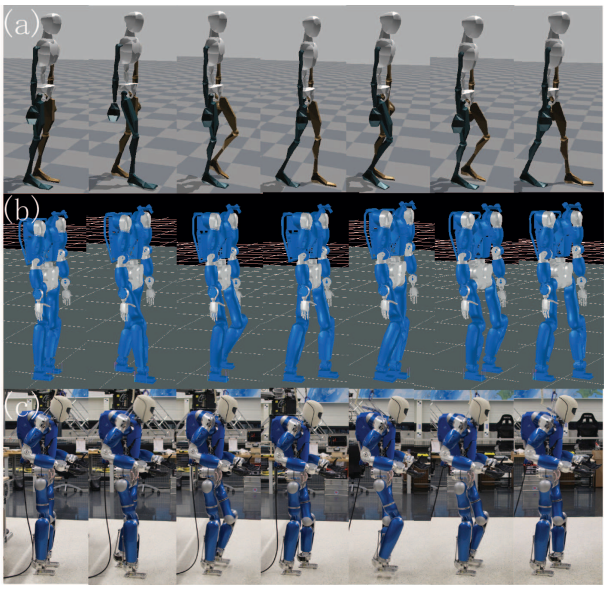

Fig. 5. Snapshots of the simulation results: (a) recorded human walking motion; (b) TORO robot imitates the human walking with larger step length (around 35cm) in simulation; (c) TORO robot imitates the human walking with smaller step length (around 20cm).

methods) are compared to show the effectiveness of the proposed approach (Fig. 6). The blue line shows the human reference knee trajectory. The green line shows the knee joint trajectory of controlling the robot to follow the recognized walking pattern using conventional ZMP-based controller, in which the COM height is fixed to be 0.92m (highest value for singularity-free walking) with fixed body orientation. The red lines show the results of proposed approach. In order to compare the differences between the human reference and robot trajectory, we calculate the mean and standard deviation of the absolute error of both knee trajectories together:

$$\mu = \frac{1}{T}\int \sum_{i=1}^{2} |e_i|\, dt \tag{16}$$

$$\sigma = \frac{1}{T}\int (\mu - \sum_{i=1}^{2} |e_i|)^2 dt \tag{17}$$

TABLE I

ABSOLUTE ERROR MEAN AND STANDARD DEVIATION OF DIFFERENT WALKING STYLES COMPARED WITH HUMAN REGARDING KNEE JOINTS.

walking style	μ	σ
walking imitation	0.2154	0.0067
conventional walking	1.1603	0.1971

The results in TABLE I show clear advance of the proposed method over the conventional method about the motion similarity measured by the knee joint angles. Since the target robot system has only flat feet, it is not capable of imitating all the contact states of the human. Bent knees are required to achieve long double support phase. This result also suggests

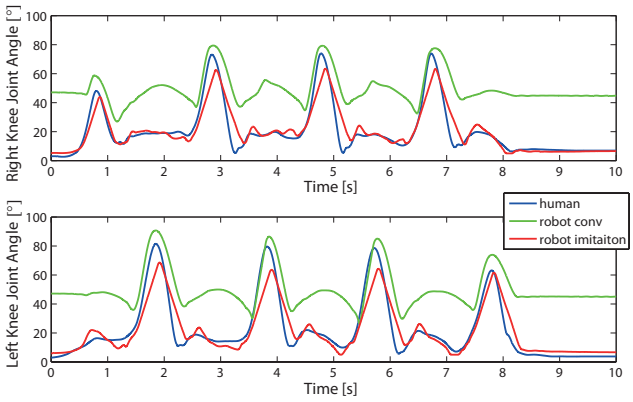

Fig. 6. Comparison of knee joint trajectories of different walking control strategies.

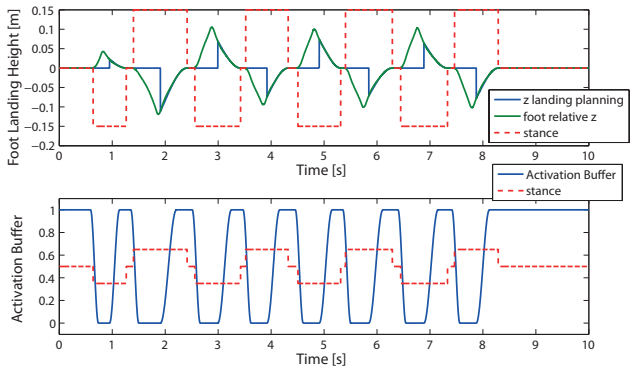

Fig. 7. State-dependent foot control: Upper-graph: The blue line shows the planned foot landing trajectory and the green line shows the real foot landing trajectory. The foot relative height is always calculated with respect to the left foot. Lower-graph: The blue line shows the activation parameter h. The transition is designed to be sinus form.

that a more human-like foot structure, such as with toe joints, can help to realize human-like walking on a humanoid robot.

B. State-dependent Foot Control

We design the activation parameter change smoothly following a sinus form. Fig. 7 shows the results of the state-dependent foot control. In the first half of the swinging phase, the robot tries to follow the knee trajectory without the foot position constraints in x and z directions. In the middle of the swing phase, a landing trajectory is planned and the foot position control constraint is added smoothly into the QP.

C. Motion Stability

There are two factors that influence the stability of the motion: the vertical COM motion and the upper body angular momentum. It has been shown in [9] that the effect of angular momentum on the ZMP deviation is much severer than the waist vertical motion. Therefore we set the weighting factor for body orientation higher than the knee tracking ($\omega_1 = 500, \omega_2 = 50$). The generated vertical COM motion has a magnitude of round 1.5cm and upper body orientation errors are within 2 degrees (Fig. 8). The real ZMP data shows that the robot can still maintain the motion stability quite well

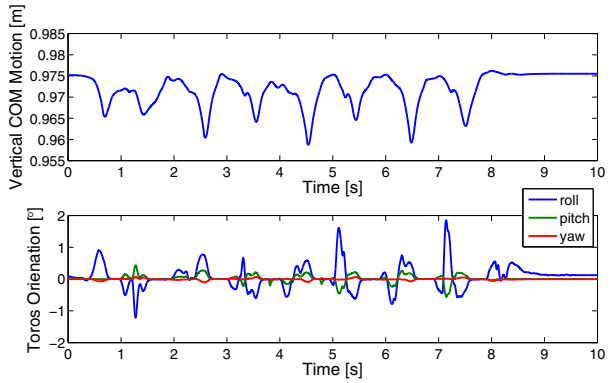

Fig. 8. Vertical COM motion and upper body orientations.

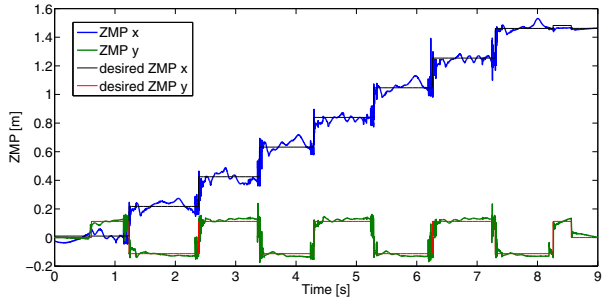

Fig. 9. ZMP data of walking imitation experiment on the real robot.

(Fig. 9). Moreover from the body orientation we can clearly observe that the robot utilizes the body roll to achieve vertical foot movements when necessary.

VI. Conclusions

In this paper we propose a novel approach for online human walking imitation in task and joint space based on quadratic programming. Besides the footprints imitation, motion similarity is considered as human knee tracking for the flat foot humanoid robot. The redundant inverse kinematics problem is formulated as a QP with dynamic equality and inequality constraints. The knee singularity is avoided by limiting the joint to a minimal safe value and treating it as an inequality constraint. Experiment results show more human-like walking motion by the proposed approach compared with the conventional ZMP based walking control.

VII. Acknowledgments

This work is supported partially by Technical University Munich - Institute for Advanced Study, funded by the German Excellence Initiative. The authors want to thank Mr. Johannes Englsberger for his help on conducting the experiment.

References

[1] N.S. Pollard, J.K. Hodgins, M.J. Riley, and C.G. Atkeson. Adapting human motion for the control of a humanoid robot. In *IEEE International Conference on Robotics and Automation*, volume 2, pages 1390–1397, 2002.

[2] S. Nakaoka, A. Nakazawa, K. Yokoi, H. Hirukawa, and K. Ikeuchi. Generating whole body motions for a biped humanoid robot from captured human dances. In *IEEE International Conference on Robotics and Automation*, volume 3, pages 3905–3910, 2003.

[3] B. Dariush, M. Gienger, Bing Jian, C. Goerick, and K. Fujimura. Whole body humanoid control from human motion descriptors. In *IEEE International Conference on Robotics and Automation*, pages 2677 –2684, May 2008.

[4] C. Ott, D. Lee, and Y. Nakamura. Motion capture based human motion recognition and imitation by direct marker control. In *8th IEEE-RAS International Conference on Humanoid Robots*, pages 399–405, 2009.

[5] K. Yamane and J. Hodgins. Control-aware mapping of human motion data with stepping for humanoid robots. In *IEEE/RSJ International Conference on Intelligent Robots and Systems*, pages 726 –733, oct. 2010.

[6] Kai Hu and Dongheui Lee. Prediction-based synchronized human motion imitation by a humanoid robot. *at-Automatisierungstechnik*, 60(11):705–714, 2012.

[7] Anirvan Dasgupta and Yoshihiko Nakamura. Making feasible walking motion of humanoid robots from human motion capture data. In *IEEE Int. Conf. on Robotics and Automation*, volume 2, pages 1044–1049. IEEE, 1999.

[8] S.K. Kim, S. Hong, and D. Kim. A walking motion imitation framework of a humanoid robot by human walking recognition from IMU motion data. In *9th IEEE-RAS International Conference on Humanoid Robots*, pages 343–348, 2010.

[9] Kensuke Harada, Kanako Miura, Mitsuharu Morisawa, Kenji Kaneko, Shinichiro Nakaoka, Fumio Kanehiro, Tokuo Tsuji, and Shuuji Kajita. Toward human-like walking pattern generator. In *IEEE/RSJ Int. Conf. on Intelligent Robots and Systems*, pages 1071–1077. IEEE, 2009.

[10] Ryo Kurazume, Shuntaro Tanaka, Masahiro Yamashita, Tsutomu Hasegawa, and Kan Yoneda. Straight legged walking of a biped robot. In *IEEE/RSJ Int. Conf. on Intelligent Robots and Systems*, pages 337–343. IEEE, 2005.

[11] Zhibin Li, Nikos G Tsagarikis, Darwin G Caldwell, and Bram Vanderborght. Trajectory generation of straightened knee walking for humanoid robot icub. In *Int. Conference on Control Automation Robotics & Vision*, pages 2355–2360. IEEE, 2010.

[12] Kanako Miura, Mitsuharu Morisawa, Fumio Kanehiro, Shuuji Kajita, Kenji Kaneko, and Kazuhito Yokoi. Human-like walking with toe supporting for humanoids. In *IEEE/RSJ Int. Conf. on Intelligent Robots and Systems*, pages 4428–4435. IEEE, 2011.

[13] Yu Ogura, Kazushi Shimomura, A Kondo, Akitoshi Morishima, Tatsu Okubo, Shimpei Momoki, Hun-ok Lim, and Atsuo Takanishi. Human-like walking with knee stretched, heel-contact and toe-off motion by a humanoid robot. In *IEEE/RSJ Int. Conf. on Intelligent Robots and Systems*, pages 3976–3981. IEEE, 2006.

[14] S. Kajita, F. Kanehiro, K. Kaneko, K. Fujiwara, K. Harada, K. Yokoi, and H. Hirukawa. Biped walking pattern generation by using preview control of zero-moment point. In *IEEE International Conference on Robotics and Automation*, volume 2, pages 1620 – 1626 vol.2, sept. 2003.

[15] Yoshihiko Nakamura and Hideo Hanafusa. Inverse kinematic solutions with singularity robustness for robot manipulator control. *ASME, Transactions, Journal of Dynamic Systems, Measurement, and Control*, 108:163–171, 1986.

[16] Oussama Kanoun, Florent Lamiraux, and P-B Wieber. Kinematic control of redundant manipulators: Generalizing the task-priority framework to inequality task. *Robotics, IEEE Transactions on*, 27(4):785–792, 2011.

[17] Y. Choi, D. Kim, Y. Oh, and B.J. You. Posture/walking control for humanoid robot based on kinematic resolution of com jacobian with embedded motion. *IEEE Transactions on Robotics*, 23(6):1285–1293, 2007.

[18] H Ferreau. qpoases–an open-source implementation of the online active set strategy for fast model predictive control. In *Proceedings of the Workshop on Nonlinear Model Based Control–Software and Applications, Loughborough*, pages 29–30, 2007.

[19] Fumio Kanehiro, Hirohisa Hirukawa, and Shuuji Kajita. Openhrp: Open architecture humanoid robotics platform. *The International Journal of Robotics Research*, 23(2):155–165, 2004.